Regular Article

Discovery of a Novel Class of State-Dependent $Na_V1.7$ Inhibitors for the Treatment of Neuropathic Pain

Kyosuke Tanaka,[a] Hiroyuki Kobayashi,[a] Sayaka Suzuki,[a] Satoshi Shibuya,[a] Hiroko Kimoto,[a,†] Yuki Domon,[a] Kazufumi Kubota,[a] Yutaka Kitano,[a] Tomihisa Yokoyama,[a] Akiko Shimizugawa,[a] Ryuta Koishi,[b] Chie Fujiwara,[a] Daigo Asano,[a] and Tsuyoshi Shinozuka*[,a]

[a] *R&D Division, Daiichi Sankyo Co., Ltd.; 1–2–58 Hiromachi, Shinagawa-ku, Tokyo 140–8710, Japan: and* [b] *Daiichi Sankyo RD Novare Co., Ltd.; 1–16–13 Kitakasai, Edogawa-ku, Tokyo 134–8630, Japan.*
Received February 12, 2020; accepted April 3, 2020

The discovery of a novel class of state-dependent voltage-gated sodium channel (Na_V)1.7 inhibitors is described. By the modification of amide or urethane bond in $Na_V1.7$ blocker III, structure–activity relationship studies that led to the identification of novel $Na_V1.7$ inhibitor 2i (DS01171986) were performed. Compound 2i exhibited state-dependent inhibition of $Na_V1.7$ without $Na_V1.1$, $Na_V1.5$ or human ether-a-go-go related gene (hERG) liabilities at concentrations up to 100 μM. Further biological profiling successfully revealed that 2i possessed potent analgesic properties in a murine model of neuropathic pain (ED_{50}: 3.4 mg/kg) with an excellent central nervous system (CNS) safety margin (> 600 fold).

Key words voltage-gated sodium channel; pain; central nervous system (CNS) side effect; quinolone; urethane

Introduction

Neuropathic pain (NP) is a debilitating disease that affects patients spontaneously and has a significant impact on their QOL. Diabetic peripheral neuropathy (DPN) is one of the most common types of NP. It is estimated that around half of diabetic patients suffer from DPN.[1)] The first-line treatments for DPN include calcium channel $\alpha_2\delta$ ligands and tricyclic antidepressants.[2)] Although these drugs are efficacious and tolerable, central nervous system (CNS) adverse effects, such as drowsiness lightheadedness, dizziness, and sedation, limit their use.[2)] Consequently, novel potent analgesic drugs with less CNS adverse effects have a high demand.

Voltage-gated sodium channels (Na_V) are responsible for transmitting neuronal signals not only in CNS but also in the peripheral nervous system (PNS). In humans, nine Na_V subtypes ($Na_V1.1$–$Na_V1.9$) have been identified, and $Na_V1.7$ has been shown to play a crucial role in pain signaling.[3,4)] Several Na_V blockers, such as lidocaine (**I**) and mexiletine (**II**) (Fig. 1), have been used to treat chronic pain in a clinical setting. Furthermore, a high safety index over CNS adverse effects is expected by selective $Na_V1.7$ inhibition, because the $Na_V1.7$ isoform is predominantly expressed in the PNS.[5)] In the discovery of novel $Na_V1.7$ inhibitors, a high subtype selectivity is crucial, because multiple Na_V subtypes are differently expressed in various organs; non-selective inhibitors could cause adverse effects. For example, $Na_V1.1$ is expressed in brain, and $Na_V1.1$ inhibition is known to cause CNS adverse effects, whereas the inhibition of $Na_V1.5$ leads to cardiac arrhythmias.[6,7)] In fact, Na_V blockers used in clinics are non-selective, and the lack of selectivity limits the usage of such drugs due to safety concerns. Therefore, the selective inhibition of $Na_V1.7$ is a promising analgesic target.[8–10)]

During the course of a project directed at acquiring potent selective $Na_V1.7$ inhibitors,[11)] we focused on benzazepinone derivative **III** (Fig. 1), reported by the Merck group, owing to its high state dependency.[12–14)] As two amide and one urethane bonds are found in this molecule, our derivatization strategy consists of the modifications of such bonds. Herein, we describe the conversion of these moieties to identify a novel class of state-dependent $Na_V1.7$ inhibitors with potent analgesic efficacy in a model of NP as well as an excellent CNS safety margin.

Results and Discussion

Human *in Vitro* Profile The *in vitro* evaluation of the compounds was performed utilizing the IonWorks Quattro automated electrophysiology platform. The inhibitory activity of $hNa_V1.7$ was evaluated at a half-inactivated state (V_{hold} −59 mV). In addition, the inhibitory potency of $hNa_V1.7$ was evaluated at an elevated membrane voltage (V_{hold} −30 mV), because an elevated $Na_V1.7$ membrane voltage is reported in damaged dorsal root ganglion (DRG) neurons.[15–18)] This screening process enabled us to provide an analgesic agent with high safety index owing to the ability to inhibit only abnormal hyperactive neurons with frequent action potentials without affecting normal firing activity. In this assay condition, we confirmed the inhibitory activity of the antiepileptic drug lacosamide, which is known to enhance slow inactivation of voltage-gated sodium channels selectively.[19)] In the *in vitro*

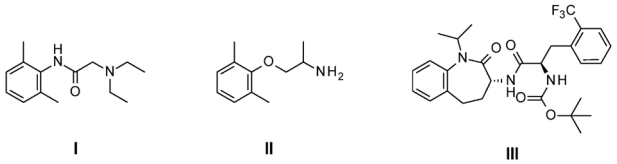

I II III

Fig. 1. Structures of Lidocaine (**I**), Mexiletine (**II**), and Compound **III**, Reported by the Merck Group

† Present address: *KAN Research Institute, Inc.; Kobe 650–0047, Japan.*

* To whom correspondence should be addressed. e-mail: sinozu.xf6@gmail.com; shinozuka.tsuyoshi.s5@daiichisankyo.co.jp

Table 1. *In Vitro* Profile of $Na_V1.7$ Inhibitors **1**[a)]

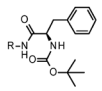

Compound	R	$hNa_V1.1$ IC_{50} (μM)[b)]	$hNa_V1.5$ IC_{50} (μM)[b)]	$hNa_V1.7$ IC_{50} (μM)[b)]	$hNa_V1.7$ IC_{50} (μM)[c)]
III		>100[e)]	>100[e)]	>100[e)]	2.5 ± 0.45
1a[d)]		32[e)]	45[e)]	72[e)]	6.9[e)]
1b		47[e)]	73[e)]	>100[e)]	3.0[e)]
1c		>100[e)]	33 ± 7.7	>100[e)]	1.6 ± 0.13
1d		>100[e)]	>100[e)]	>100[e)]	9.1[e)]
1e		>100[e)]	36[e)]	>100[e)]	4.8[e)]
1f		17[e)]	32[e)]	>100[e)]	1.4[e)]
1g		>100[e)]	>100[e)]	>100[e)]	5.2 ± 0.33
1h		51[e)]	16[e)]	68[e)]	8.1[e)]

a) Values of at least two independent experiments run in quadruplicate, unless otherwise noted. Each value represents the mean ± standard error of the mean (S.E.M.) *b*) Values at a half-inactivated state. *c*) Values at V_{hold} −30 mV. *d*) Diastereomeric mixture (1 : 1). *e*) Values of a single experiment run in quadruplicate.

screening, $hNa_V1.1$ and $hNa_V1.5$ inhibitory activities were acquired to monitor adverse effects.

We initially focused on the conversion of the benzazepinone moiety, as shown in Table 1. Compound **III** showed good inhibitory potency against $hNa_V1.7$ at V_{hold} −30 mV ($IC_{50} = 2.5\,\mu M$) without $hNa_V1.1$ or $hNa_V1.5$ liability. Compound **III** was found to inhibit $hNa_V1.7$ in a high state-dependent manner, because **III** did not inhibit $hNa_V1.7$ at a half-inactivated state. As the removal of the trifluoromethyl group or the reduction of ring size (benzazepinone to dihydroquinolinone) did not affect $hNa_V1.7$ potency (data not shown), tetrahydroquinoline **1a** was synthesized, which resulted in the retention of $hNa_V1.7$ potency. Compound **1a** was prepared as a diastereomeric mixture (1 : 1). These results encouraged us to synthesize quinoline and isoquinoline derivatives. As expected, isoquinoline **1b** and quinoline **1c** exhibited potent $hNa_V1.7$ activity. Compounds **1b** and **1c** also showed no $hNa_V1.1$ or $hNa_V1.5$ liabilities. As other regioisomers of **1b** and **1c** did not show potent inhibitory activity (data not shown), alternative heteroaromatic rings were investigated. 2-Benzoazoles such as **1d**, **1e** and **1f** retained $hNa_V1.7$ activity. In particular, 2-benzimidazole **1f** exhibited the best inhibitory potency among this series of compounds with increased $hNa_V1.1$ or $hNa_V1.5$ potency. In contrast to quinolone derivatives, the regioisomer of **1d**, 5-benzothiazole **1g** retained $hNa_V1.7$ potency without $hNa_V1.1$ or $hNa_V1.5$ liabilities. Although the enhancement of $hNa_V1.7$ activity was expected by the introduction of a nitrogen in **1g**, thiazolopyridine **1h** showed attenuated $hNa_V1.7$ potency.

The replacement of acid labile Boc group of **1c** was then investigated (Table 2). $hNa_V1.7$ activity was found to be correlated to the lipophilicity of molecules in the modification of *t*-butyl group. The inhibitory activity of isopropyl **2a** and ethyl derivative **2b** is 2.3 and 10 μM, respectively, whereas methyl analog **2c** almost lost activity. Consequently, *t*-butyl group was optimal in this position. The introduction of methyl group in the urethane moiety led to the loss of potency *in vitro*, suggesting that a hydrogen bond may exist between this moiety and the ion channel (compound **2d**). The importance of this hydrogen bond network was confirmed by amide derivatives, because *β*-alanine **2e** and neopentyl amide **2g** lost potency, whereas neopentyl amide **2f** maintained the activity. As the hydrogen bond donor exists in this position,

Table 2. *In Vitro* Profile of $Na_V1.7$ Inhibitors **2**[a)]

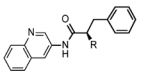

Compound	R	$hNa_V1.1$ IC_{50} (μM)[b)]	$hNa_V1.5$ IC_{50} (μM)[b)]	$hNa_V1.7$ IC_{50} (μM)[b)]	$hNa_V1.7$ IC_{50} (μM)[c)]
2a		>100[e)]	9.9 ± 2.1	48[e)]	2.3[e)]
2b		>100[e)]	33 ± 13	>100[e)]	10[e)]
2c		>100[e)]	24[e)]	>100[e)]	86[e)]
2d		>100[e)]	NT[f)]	NT[f)]	>100[e)]
2e[d)]		>100[e)]	35[e)]	NT[f)]	>100[e)]
2f		67[e)]	75[e)]	80[e)]	3.4[e)]
2g[d)]		>100[e)]	NT[f)]	NT[f)]	>100[e)]
2h		>100[e)]	>100[e)]	>100[e)]	13[e)]
2i		>100[e)]	>100[e)]	>100[e)]	5.2 ± 2.0

a) Values of at least two independent experiments run in quadruplicate unless otherwise noted. Each value represents the mean ± S.E.M. *b*) Values at a half-inactivated state. *c*) Values at V_{hold} −30 mV. *d*) Racemic mixture. *e*) Values of a single experiment run in quadruplicate. *f*) Not tested.

urea **2h** maintained the activity. Compounds **2e** and **2g** were prepared as a racemic mixture. Reverse urethane **2i** displayed decent $hNa_V1.7$ potency ($IC_{50} = 5.2\,\mu M$), and **2i** did not exhibit $hNa_V1.1$ or $hNa_V1.5$ liabilities at concentrations up to 100 μM.

Mice *in Vitro* Profile, *in Vitro* ADME Properties, and Pharmacokinetics (PK) Parameters in Mice Potent compounds without $hNa_V1.1$ or $hNa_V1.5$ liabilities were evaluated for mouse Na_V activities, *in vitro* ADME properties and PK parameters in mice as shown in Table 3. To evaluate the state dependency, $mNa_V1.7$ activity at V_{hold} −30 mV was measured, and all selected compounds exhibited comparable mouse i*n vitro* profiles to that of human.[20)] Compounds **1c**, **1g**, and **2i** exerted high membrane permeability in Parallel Artificial Membrane Permeation Assay (PAMPA) and were expected to exhibit high plasma exposure in the PK study. Compound **1b** lacked adequate aqueous solubility, whereas better solubility was observed in other compounds. Additionally, all evaluated compounds exhibited acceptable plasma protein binding (PB) ability (free fraction >1.0%). PK parameters were acquired by orally administering the compounds to mice at 30 mg/kg. Compounds **1b** and **1c** showed poor plasma exposure of the test compound, whereas a slight improvement of the PK profile was observed in reverse urethane **2i**. Further improvement of the plasma exposure was observed in benzothiazole **1g**. Considering the mouse *in vitro* activity, plasma PB ability, and PK parameters, **1g** was expected to exhibit potent efficacy. In the PK evaluation, all evaluated compounds exhibited T_{max} less than 1 h, which would be expected immediate onset of pharmacological efficacy *in vivo*.

To unveil the brain penetration of the compound, the *K*p brain value of **1c** and **2i** was assessed. After 0.5 h of the compound administration (30 mg/kg, *p.o.*), the brain concentration of the compounds was determined ($n = 2$). Compound **2i** indicated less exposure in the brain than in the plasma, while higher brain concentration of **1c** was observed.

***In Vivo* Efficacy** The assessment of *in vivo* efficacy was conducted on thermal hyperalgesia in mice evoked by partial sciatic nerve ligation (PSL, Seltzer), a model of NP[21)] (Fig. 2). The model was prepared by partial ligation of 1/2 to 1/3 of the left sciatic nerve with silk suture. The paw withdrawal latency (PWL, second) was assessed after 30, 60, 120, and 180 min of oral administration of the test compound (Plantar

Table 3. Mouse Na_V IC_{50} Values, *in Vitro* ADME Properties and PK Parameters

Compound		1b	1c	1g	2i
$mNa_V1.1$ IC_{50} (μM)[a,b]		18[h]	29 ± 8.4	>100[h]	>100[h]
$mNa_V1.5$ IC_{50} (μM)[a,b]		43[h]	43 ± 12	>100[h]	>100[h]
$mNa_V1.7$ IC_{50} (μM)[a,b]		>100[h]	>100[h]	>100[h]	>100[h]
$mNa_V1.7$ IC_{50} (μM)[a,c]		4.3[h]	2.0 ± 0.24	4.8 ± 0.70	11.8 ± 2.2
PAMPA P_{app} (10^{-6} cm/s)[d]		NT[i]	>50	>50	>50
Solubility (μg/mL)[e]		1.4	23	28	17
PB free (%)[f]		2.54	2.72	3.04	1.04
PK parameters in ddY mice at 30 mg/kg[g]	C_{max} (μg/mL)	0.010 ± 0.0036	0.032 ± 0.0077	1.45 ± 0.090	0.10 ± 0.019
	T_{max} (h)	0.67 ± 0.29	0.67 ± 0.29	0.50 ± 0.00	0.50 ± 0.00
	AUC_{0-24h} (h·μg/mL)	0.031 ± 0.020	0.051 ± 0.011	2.84 ± 0.24	0.20 ± 0.047
	$T_{1/2}$ (h)	1.4 ± 0.47	1.1 ± 0.53	6.0 ± 2.4	6.8 ± 3.3
	K_p Brain	NT[i]	1.65	NT[i]	0.69

a) Values of at least two independent experiments run in quadruplicate unless otherwise noted. Each value represents the mean ± S.E.M. *b*) Values at a half-inactivated state. *c*) Values at V_{hold} −30 mV. *d*) PAMPA was performed at pH 7.4. Values of a single experiment run in duplicate. *e*) Aqueous thermodynamic solubility at pH 6.8. Values of a single experiment run in duplicate. *f*) Unbound fractions (%) in mouse plasma. *g*) Average of three male ddY mice dosed at 30 mg/kg *per os* (*p.o.*) in *N*,*N*-dimethylacetamide/Tween80/saline: 10/10/80. *h*) Values of a single experiment run in quadruplicate. *i*) Not tested.

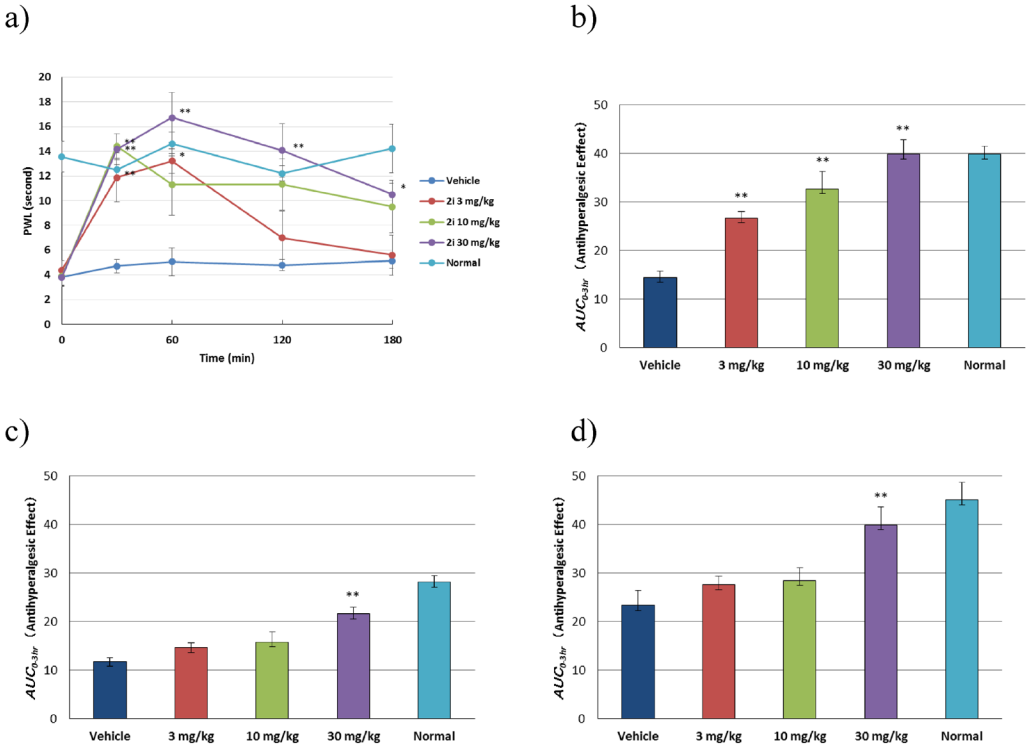

Fig. 2. Dose–Response Effect on Thermal Hyperalgesia (Plantar Test) in PSL Model of NP (Seltzer)

Compound **2i** was administrated by po route in *N*,*N*-dimethylacetamide/Tween80/saline: 10/10/80 ($n = 5$). (a) Time course of PWL (second). (b) AUC_{0-3h} of each curve in Fig. 2a (antihyperalgesic effect of **2i**). (c) antihyperalgesic effect of **1c** ($n = 6$). (d) antihyperalgesic effect of **1g** ($n = 5$). Each value is the mean ± S.E.M. Statistical significance compared to vehicle treatment is denoted by * ($p < 0.05$), and ** ($p < 0.01$) as determined by the Dunnett multiple comparison test. (Color figure can be accessed in the online version.)

test). Compared with the normal group, the pain threshold was significantly lowered in the operated group, indicating the development of hyperalgesia. The time course of the efficacy of compound **2i** administered to PSL mice is shown in Fig. 2a. The administration of **2i** at 3 mg/kg *p.o.* (red curve) reversed the thermal PWL from 30 to 120 min. This reversal of hyperalgesia was maximized significantly from 30 to 60 min ($p < 0.01$ at 30 min, and $p < 0.05$ at 60 min). The peak efficacy improved PWL to almost normal levels. The therapeutic efficacy of **2i** at 3 mg/kg was maximized from 30 to 60 min, whereas the plasma concentration of **2i** at 30 mg/kg peaked at 30 min in the PK study. The thermal hyperalgesia was suppressed in a dose dependent manner (3, 10, and 30 mg/kg), and the administration of **2i** at 30 mg/kg significantly reversed hyperalgesia at all timepoints evaluated (purple curve, $p < 0.01$ from 30 to 120 min, and $p < 0.05$ at 180 min). Potent analgesic efficacy lasted until 180 min when 10 or 30 mg/kg of **2i** was administered. The retention of potent efficacy at 30 mg/kg administered group correlates with the PK parameters, because $T_{1/2}$ of **2i** at 30 mg/kg was 6.8 h (Table 3). AUC_{0-3h} (area under curve for 0–3 h) for each curve was calculated to analyze the total anti-hyperalgesic effect (Fig. 2b). The anti-hyperalgesic

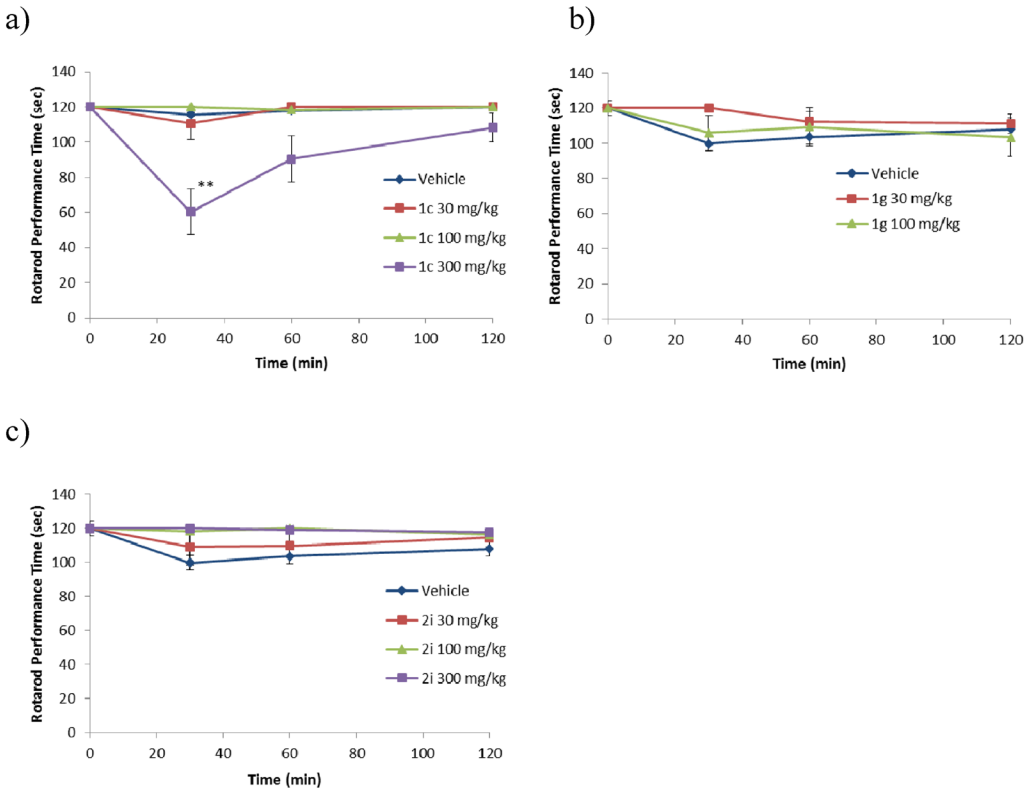

Fig. 3. Dose–Response Effects of Compounds **1c** (a), **1g** (b), and **2i** (c) on Motor Coordination in ddY Mice (Rotarod Test, $n = 10$)

Each value is the mean ± S.E.M. Statistical significance compared to vehicle treatment is denoted by ** ($p < 0.01$) as determined by the Steel–Dwass test. (Color figure can be accessed in the online version.)

Table 4. TK Parameters, Thermal Hyperalgesia ED_{50} Values, Rotarod ID_{50} Values and CNS Safety Margin

Compound	TK parameters in ddY mice[a)]				Thermal hyperalgesia ED_{50}[b)] (mg/kg)	Rotarod ID_{50}[c)] (mg/kg)	CNS safety margin[d)]
	Dose (mg/kg)	T_{max} (h)	C_{max} (μg/mL)	AUC_{all} (h·μg/mL)			
1c	300[e)]	1.0[e)]	2.56[e)]	4.49[e)]	23	>300	>100
1g	100	0.50 ± 0.00[f)]	6.63 ± 0.87[f)]	15.2 ± 1.4[f)]	16	>100	>8.6
2i	300	1.0 (1.0, 1.0)[g)]	6.77 (7.65, 5.89)[g)]	15.0 (13.7, 16.3)[g)]	3.4	>300	>600

a) Average of ddY mice dosed at 100 or 300 mg/kg po in *N*,*N*-dimethylacetamide/Tween80/saline: 10/10/80 ($n = 1$–3). *b*) The ED_{50} value was calculated from the suppression of thermal pain behavior in PSL mice after oral administration of compounds (Fig. 2). *c*) The ID_{50} value was calculated from the effect on motor coordination (Fig. 3). *d*) CNS safety margin = Calculated C_{max} at rotarod ID_{50} in TK study/calculated C_{max} at Plantar ED_{50} in PK study. *e*) $n = 1$. *f*) $n = 3$. *g*) Individual data ($n = 2$).

effect occurred in a clear dose dependent manner, and ED_{50} of **2i** was estimated to be 3.4 mg/kg. Compound **2i** at 30 mg/kg significantly improved the total hyperalgesic effect to the normal levels ($p < 0.01$).

Isoquinoline **1b** failed to show potent efficacy on thermal hyperalgesia at 30 mg/kg (data not shown), owing to less plasma exposure of **1b**, as suggested by the PK study. The total anti-hyperalgesic effect of **1c** and **1g** is shown in Figs. 2c and 2d. Compound **1c** suppressed thermal hyperalgesia in a dose-dependent manner (3, 10, 30 mg/kg), and ED_{50} was estimated to be 23 mg/kg. Although a remarkable improvement in PK parameters was observed in 5-benzothiazole **1g**, the efficacy of **1g** in PSL mice was comparable to that of **1c**, with $ED_{50} = 16$ mg/kg. There was a difference observed in AUC_{0-3h} of control groups (vehicle-treated and normal groups) in Figs. 2b, 2c, and 2d. AUC_{0-3h} of control groups in Fig. 2d is higher than those in Figs. 2b and 2c. Consequently, the pain threshold of the study with **1g** is higher than those with **2i** and **1c**. As ED_{50} value is calculated defined PWL of vehicle-treated group as 0%, and PWL of normal mice as 100%, the inter-assay variation in pain threshold has no significant influence on ED_{50}.

Toxicological Evaluation Compounds with potent analgesic efficacy (**1c**, **1g**, and **2i**) were selected for CNS toxicological evaluation as indicated in Fig. 3. The *in vivo* CNS side effects were assessed using a mice rotarod test, a model of motor coordination at 30, 100, and 300 mg/kg ($n = 10$). TK parameters were acquired at 100 or 300 mg/kg from a satellite group (Table 4, $n = 1 - 3$). As the administration of compound **1g** at 300 mg/kg was lethal (two mice died after 120 min), the results of rotarod test are shown in 30 and 100 mg/kg administered group (Fig. 2b). The administration of **1g** at 30 or 100 mg/kg did not effect on rotarod activity in mice, and $ID_{50}$was calculated to be >100 mg/kg. Compared to anti-thermal hyperalgesia efficacy, plasma-exposure-based CNS safety margin of **1g** was determined to be >8.6-fold (Table 4). On

the contrary, two other compounds, **1c** and **2i**, demonstrated superior CNS safety properties. Although 300 mg/kg administration of compound **1c** significantly affected the results of rotarod test at 30 min ($p < 0.01$), this side effect was attenuated at 120 min ($ID_{50} > 300$ mg/kg). Consequently, the plasma exposure-based CNS safety margin of **1c** was determined to be >100-fold. Furthermore, the administration of **2i** at 300 mg/kg did not affect mice motor activity at all timepoints with $ID_{50} > 300$ mg/kg. Consequently, the plasma exposure-based CNS safety margin of **2i** was >600-fold.

With promising results, **2i** was further evaluated. An *in vitro* assessment established that **2i** did not inhibit other related ion channels, including human $Na_V1.2$, 1.3, 1.4, 1.6, or human ether-a-go-go related gene (hERG). Moreover, *in vitro* pharmacological activity of **2i** on a total of 67 receptors, channels, and transporters was evaluated; **2i** inhibited adenosine A1 and serotonin 5-HT2B by 50% at 10 μM.[22] These data indicate that **2i** is a selective $Na_V1.7$ inhibitor *in vitro*.

Conclusion

The discovery of quinoline amides as a novel class of state-dependent $Na_V1.7$ inhibitors has been described. The benzazepinone moiety of compound **III** was replaced with a heteroaromatic ring. Among a variety of heteroaromatic rings examined, quinoline ring was shown to be optimal regarding potency as well as $Na_V1.1$ or $Na_V1.5$ liabilities. The modification of acid-unstable Boc group led to the discovery of reverse urethane **2i** (DS01171986). Compound **2i** inhibited $hNa_V1.7$ at $IC_{50} = 5.2\,\mu$M in a state-dependent manner. Notably, **2i** inhibited $Na_V1.7$ without affecting other receptors, channels, and transporters, including other Na_V subtypes and hERG. Compound **2i** demonstrated potent analgesic efficacy in NP model with $EC_{50} = 3.4$ mg/kg. A CNS adverse effect evaluation revealed that **2i** possessed excellent CNS safety margin (>600 fold).

Experimental

General Starting reagents were purchased from commercial suppliers and were used without further purification unless otherwise specified. Chromatographic elution was carried under continuous monitoring by TLC using silica gel 60F254 (Merck & Co., Inc., Germany) as the stationary phase; the mobile phase was the elution solvent used in column chromatography. A UV detector was used for detection. Silica gel SK-85 (230–400 mesh) or silica gel SK-34 (70–230 mesh), manufactured by Merck & Co., Inc., or Chromatorex NH (200–350 mesh), manufactured by Fuji Silysia Chemical Ltd. (Japan), was used as the column packing silica gel. ^{1}H-NMR spectra were obtained on Varian Unity 400- and 500-MHz spectrometers. Spectra were recorded in the indicated solvent at ambient temperature; chemical shifts are reported in ppm (δ) relative to the solvent peak. Resonance patterns are represented with the following notations: br (broad signal), s (singlet), d (doublet), t (triplet), q (quartet) and m (multiplet). MS analysis was carried out by FAB, electron ionization (EI), or electrospray ionization (ESI). High resolution (HR)MS was carried out using an LC-MS system composed of a Waters Xevo Q-ToF MS and an Acquity UHPLC system. Elemental analyses were carried out on a Microcorder JM10 and a Dionex ICS-1500. The purity of compounds was confirmed as over 95% by diode array detector (DAD) signal area% performed on Agilent Infinity 1260 LCMS system. Conditions [column: Develosil Combi-RP-5 2.0 mmID × 50 mmL, gradient elution: 0.1% HCO_2H–H_2O/0.1% HCO_2H–MeCN = 98/2 to 0/100 (v/v), flow rate: 1.2 mL/min, UV detection: 254 nm, column temperature: 40°C, ionization: APCI/ESI].

Chemical Synthesis Compounds **1a**–**h** listed in Table 1 were synthesized by amidation of corresponding amine with *N*-Boc-D-phenylalanine under usual reaction conditions (Chart 1). The synthesis of thiazolopyridine **7** for **1h** was accomplished by the annulation of chloropyridine **5** as a key step.[23]

Chart 2 summaries the preparation of compounds **2a**–**i** listed in Table 3. Compounds **2a**–**2c** and **2f** were synthesized from amine **8** derived from **1c** by the reaction with carbonyl chlorides, whereas urea **2h** was prepared from **8** reacted with *tert*-butyl isocyanate. *N*-Methyl urethane **2d** was prepared by the condensation of 3-aminoquinoline with *N*-methyl-*N*-Boc-D-phenylalanine (structures not shown). The synthesis of β-alanine **2e** was achieved from key intermediate **11**, which was prepared from benzyl alcohol **10** and *tert*-butyl bromoacetate.[24] Started from **15**,[25] neopentyl amide **2g** was synthesized in a similar manner. Reverse urethane **2i** was prepared from D-phenyllactic acid **18**.

General Procedure for Amidation (General Procedure A) A solution of amine (3.47 mmol), carboxylic acid (3.47 mmol), *N*,*N*-diisopropylethylamine (DIPEA) (2.7 mL, 15.6 mmol), *N*-hydroxybenzotriazole (HOBt)·H_2O (0.84 g, 6.24 mmol) and WSC·HCl (1.20 g, 6.24 mmol) in tetrahydrofuran (THF) (23 mL) was stirred at room temperature overnight under N_2. Water was added to the reaction mixture, and the mixture was extracted with EtOAc several times. The combined organic layer was dried over anhydrous Na_2SO_4 and concentrated under reduced pressure. The residue was purified by silica gel chromatography to obtain **1**.

General Procedure for Amidation to Prepare 2 (General Procedure B) A solution of amine **3** (70 mg, 0.24 mmol) and

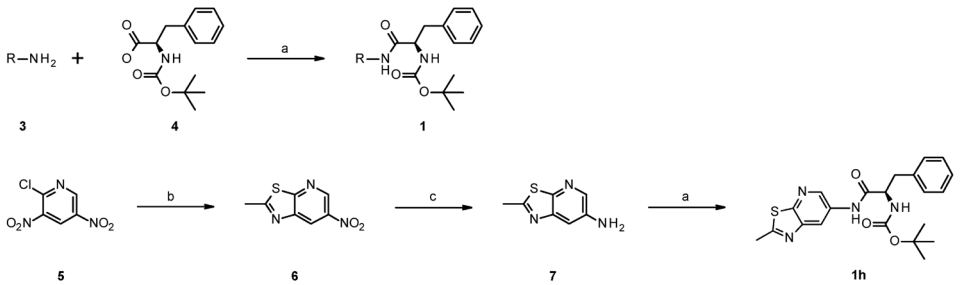

Reagents and conditions: (a) WSC·HCl, HOBt, DIPEA, THF; (b) thioacetamide, 1,4-dioxane, 100°C, 27%; (c) Fe, HCl, EtOH, H_2O.

Chart 1. Synthesis of Compounds **1a**–**h**

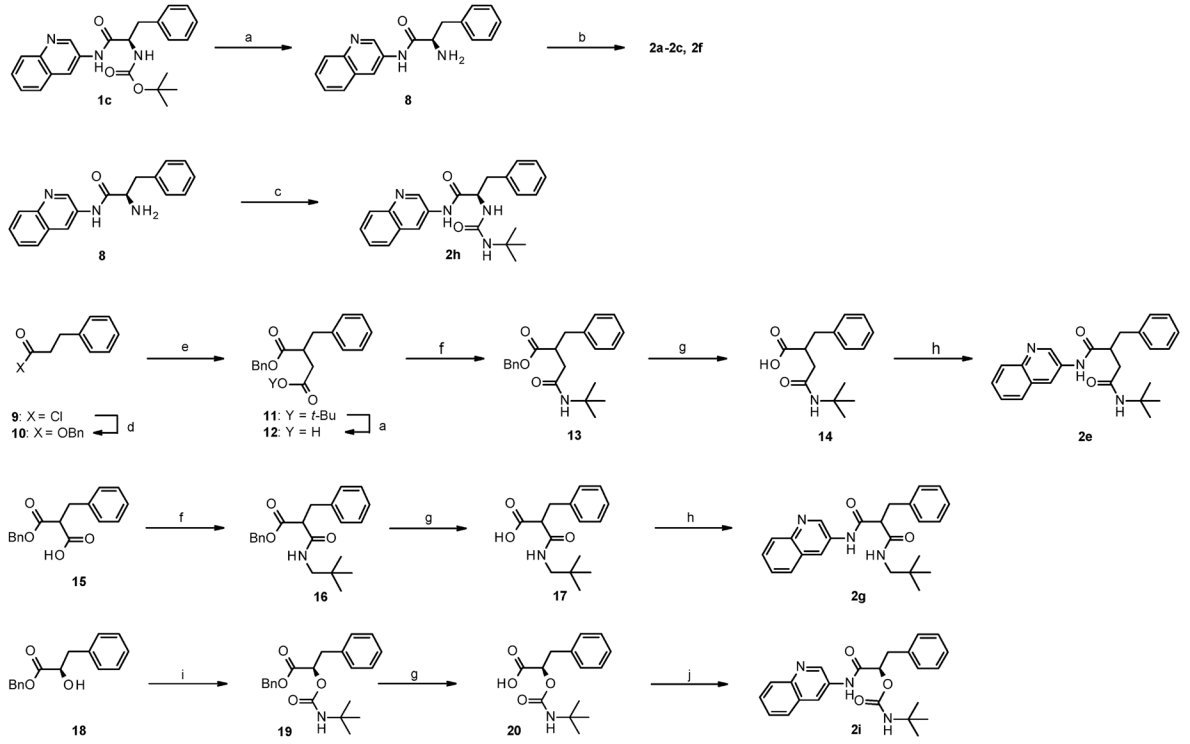

Reagents and conditions: (a) TFA, CH_2Cl_2; (b) RCOCl, Et_3N, CH_2Cl_2; (c) *tert*-butyl isocyanate, toluene, 77%; (d) BnOH, Et_3N, CH_2Cl_2, 91%; (e) *tert*-butyl bromoacetate, LDA, THF, −78°C, 56%; (f) *tert*-butylamine or neopentylamine, WSC·HCl, HOBt, CH_2Cl_2; (g) H_2, Pd/C, EtOH; (h) 3-aminoquinoline, WSC·HCl, HOBt, CH_2Cl_2; (i) *tert*-butyl isocyanate, Me_3SiCl, CH_2Cl_2; (j) 3-aminoquinoline, HATU, DMF, 45%.

Chart 2. Synthesis of Compounds **2a**–**i**

Et_3N (0.10 mL, 0.72 mmol) in CH_2Cl_2 (1.2 mL) was added chloroformate or acid chloride (0.57 mmol) at room temperature under N_2. After being stirred at room temperature for several hours, the mixture was directly purified by silica gel chromatography to obtain **2a–2c** or **2f**.

General Procedure for Deprotection by Hydrogenolysis (General Procedure C) A solution of benzyl ester (3.72 mmol) and Pd/C (10%, 300 mg) in EtOH (10 mL) was stirred at room temperature under H_2 for several hours. After the removal of the catalyst, the residue was concentrated to obtain carboxylic acid.

***tert*-Butyl[(2*R*)-1-oxo-3-phenyl-1-(1,2,3,4-tetrahydroquinolin-3-ylamino)propan-2-yl]carbamate (1a)** Prepared according to General Procedure A as a diastereomeric mixture. Yield: 99%. HRMS (ESI) *m/z*: $[M+H]^+$ calcd for $C_{23}H_{30}N_3O_3$, 396.2293; found 396.2289.

***tert*-Butyl[(2*R*)-1-(isoquinolin-3-ylamino)-1-oxo-3-phenylpropan-2-yl]carbamate (1b)** Prepared according to General Procedure A. Yield: 63%. ^{1}H-NMR (400 MHz, $CDCl_3$) δ: 1.42 (9H, s), 3.11–3.20 (1H, m), 3.27 (1H, dd, $J=6.3$, 14.1 Hz), 4.64 (1H, s), 5.18 (1H, d, $J=7.0$ Hz), 7.19–7.29 (5H, m), 7.48 (1H, t, $J=6.7$ Hz), 7.64 (1H, t, $J=7.0$ Hz), 7.83 (1H, d, $J=8.2$ Hz), 7.87 (1H, d, $J=8.2$ Hz), 8.58 (1H, s), 8.69 (1H, s), 8.94 (1H, s); MS (APCI/ESI) *m/z*: 392 $[M+H]^+$; *Anal.* calcd for $C_{23}H_{25}N_3O_3$: C, 70.57; H, 6.44; N, 10.73. Found C, 70.49; H, 6.62; N, 10.91; $[\alpha]_D^{25}$ +6.85 ($c=0.974$, $CHCl_3$).

***tert*-Butyl[(2*R*)-1-oxo-3-phenyl-1-(quinolin-3-ylamino)-propan-2-yl]carbamate (1c)** Prepared according to General Procedure A. Yield: 45%. ^{1}H-NMR (400 MHz, $CDCl_3$) δ: 1.43 (9H, s), 3.14 (1H, dd, $J=7.4$, 14.1 Hz), 3.21 (1H, dd, $J=7.4$, 14.1 Hz), 4.64 (1H, s), 5.39 (1H, d, $J=7.8$ Hz), 7.21–7.30 (5H, m), 7.45 (1H, t, $J=7.2$ Hz), 7.56 (1H, t, $J=7.8$ Hz), 7.66 (1H, d, $J=7.4$ Hz), 7.95 (1H, d, $J=8.6$ Hz), 8.53 (1H, d, $J=2.3$ Hz), 8.58 (1H, s), 8.78 (1H, s); MS (APCI/ESI) *m/z*: 392 $[M+H]^+$; *Anal.* calcd for $C_{23}H_{25}N_3O_3$: C, 70.57; H, 6.44; N, 10.73. Found C, 70.40; H, 6.61; N, 10.75; $[\alpha]_D^{25}$ +5.92 ($c=0.980$, $CHCl_3$).

***N*-1,3-Benzothiazol-2-yl-*Nα*-(*tert*-butoxycarbonyl)-D-phenylalaninamide (1d)** Prepared according to General Procedure A. Yield: 90%. ^{1}H-NMR (400 MHz, $CDCl_3$) δ: 1.40 (9H, s), 3.08–3.16 (1H, m), 3.22 (1H, dd, $J=6.0$, 14.4 Hz), 4.74 (1H, s), 5.19 (1H, s), 7.07–7.13 (2H, m), 7.18–7.25 (3H, m), 7.32 (1H, t, $J=6.8$ Hz), 7.43 (1H, t, $J=8.4$ Hz), 7.76 (1H, d, $J=8.0$ Hz), 7.83 (1H, d, $J=8.0$ Hz); MS (APCI/ESI) *m/z*: 398 $[M+H]^+$; *Anal.* calcd for $C_{21}H_{23}N_3O_3S\cdot 0.20H_2O$: C, 62.89; H, 5.88; N, 10.48. Found C, 62.84; H, 5.83; N, 10.56; $[\alpha]_D^{25}$ +59.9 ($c=1.007$, $CHCl_3$).

***N*-1,3-Benzoxazol-2-yl-*Nα*-(*tert*-butoxycarbonyl)-D-phenylalaninamide (1e)** Prepared according to General Procedure A. Yield: 50%. ^{1}H-NMR (400 MHz, $CDCl_3$) δ: 1.41 (9H, s), 3.13 (1H, s), 3.28 (1H, dd, $J=5.9$, 14.1 Hz), 4.69 (1H, s), 5.14 (1H, s), 7.20–7.32 (8H, m), 7.45 (1H, d, $J=8.2$ Hz); MS (APCI/ESI) *m/z*: 382 $[M+H]^+$; *Anal.* calcd for $C_{21}H_{23}N_3O_4\cdot 0.10H_2O$: C, 65.82; H, 6.10; N, 10.96. Found C, 65.69; H, 6.19; N, 10.82; $[\alpha]_D^{25}$ +14.0 ($c=1.007$, $CHCl_3$).

***Nα*-(*tert*-Butoxycarbonyl)-*N*-(1-methyl-1*H*-benzimidazol-2-yl)-D-phenylalaninamide (1f)** Prepared according to General Procedure A. Yield: 30%. ^{1}H-NMR (400 MHz, $CDCl_3$) δ: 1.45 (9H, s), 3.25 (2H, t, $J=5.3$ Hz), 3.61 (3H, s), 4.62–4.67 (1H, m), 5.43 (1H, d, $J=7.0$ Hz), 7.17–7.31 (9H, m); MS (APCI/ESI) *m/z*: 395 $[M+H]^+$; *Anal.* calcd for $C_{22}H_{26}N_4O_3\cdot 0.10H_2O$: C, 66.68; H, 6.66; N, 14.14. Found C, 66.56; H, 6.58; N, 14.16; $[\alpha]_D^{25}$ +73.9 ($c=0.740$, $CHCl_3$).

***Nα*-(*tert*-Butoxycarbonyl)-*N*-(2-methyl-1,3-benzothiazol-5-yl)-D-phenylalaninamide (1g)** Prepared according to General Procedure A. Yield: 88%. ^{1}H-NMR (400 MHz, $CDCl_3$) δ: 1.44 (9H, s), 2.82 (3H, s), 3.12–3.20 (2H, m), 4.46 (1H, br), 5.14 (1H, br), 7.26–7.34 (5H, m), 7.45 (1H, dd, J = 2.0, 8.6 Hz), 7.71 (1H, d, J = 8.6 Hz), 7.80 (1H, br), 7.91 (1H, d, J = 2.0 Hz); HRMS (ESI) m/z: $[M+H]^+$ calcd for $C_{22}H_{26}N_3O_3S$, 412.1690; found 412.1709; *Anal.* calcd for $C_{22}H_{25}N_3O_3S$: C, 64.21; H, 6.12; N, 10.21. Found C,63.92; H, 6.36; N, 10.13; $[\alpha]_D^{25}$ +4.23 (c = 1.003, $CHCl_3$).

***Nα*-(*tert*-Butoxycarbonyl)-*N*-(2-methyl[1,3]thiazolo[5,4-*b*]pyridin-6-yl)-D-phenylalaninamide (1h)** Prepared according to General Procedure A. Yield: 46% (2 steps). ^{1}H-NMR (400 MHz, $CDCl_3$) δ: 1.45 (9H, s), 2.85 (3H, s), 3.13–3.25 (2H, m), 4.46–4.54 (1H, m), 5.13 (1H, br), 7.26–7.36 (5H, m), 7.99 (1H, br), 8.39 (1H, d, J = 2.3 Hz), 8.44 (1H, d, J = 2.0 Hz); HRMS (ESI) m/z: $[M+H]^+$ calcd for $C_{21}H_{25}N_4O_3S$, 413.1642; found 413.1648; $[\alpha]_D^{25}$ +4.4 (c = 0.302, $CHCl_3$).

Propan-2-yl[(2*R*)-1-oxo-3-phenyl-1-(quinolin-3-ylamino)-propan-2-yl]carbamate (2a) Prepared as a mixture of conformers according to General Procedure B utilizing isopropyl chloroformate as an acylating reagent. Yield: 46%. HRMS (ESI) m/z: $[M+H]^+$ calcd for $C_{22}H_{24}N_3O_3$, 378.1823; found 378.1810; $[\alpha]_D^{25}$ +5.9 (c = 0.304, $CHCl_3$).

Ethyl[(2*R*)-1-oxo-3-phenyl-1-(quinolin-3-ylamino)propan-2-yl]carbamate (2b) Prepared as a mixture of conformers according to General Procedure B utilizing ethyl chloroformate as an acylating reagent. Yield: 80%. MS (APCI/ESI) m/z: 364 $[M+H]^+$; *Anal.* calcd for $C_{21}H_{21}N_3O_3 \cdot 0.50H_2O$: C, 67.73; H, 5.95; N, 11.28. Found C, 67.77; H, 5.79; N, 11.26; $[\alpha]_D^{25}$ +2.6 (c = 1.002, $CHCl_3$).

Methyl[(2*R*)-1-oxo-3-phenyl-1-(quinolin-3-ylamino)propan-2-yl]carbamate (2c) Prepared according to General Procedure B utilizing methyl chloroformate as an acylating reagent. Yield: 96%. ^{1}H-NMR (400 MHz, $CDCl_3$) δ: 3.16 (1H, dd, J = 7.4, 13.7 Hz), 3.26 (1H, dd, J = 6.7, 13.7 Hz), 3.73 (3H, s), 4.56–4.62 (1H, m), 5.37 (1H, s), 7.25–7.35 (5H, m), 7.52–7.55 (1H, m), 7.61–7.66 (1H, m), 7.79 (1H, d, J = 8.2 Hz), 8.02 (1H, d, J = 8.6 Hz), 8.51 (1H, d, J = 2.7 Hz), 8.64 (1H, d, J = 2.3 Hz); HRMS (ESI) m/z: $[M+H]^+$ calcd for $C_{20}H_{20}N_3O_3$, 350.1510; found 350.1504; $[\alpha]_D^{25}$ +6.2 (c = 0.306, $CHCl_3$).

***tert*-Butyl Methyl[(2*R*)-1-oxo-3-phenyl-1-(quinolin-3-ylamino)propan-2-yl]carbamate (2d)** Prepared according to General Procedure A utilizing *N*-(*tert*-butoxycarbonyl)-*N*-methyl-D-phenylalanine as a starting material. Yield: 99%. ^{1}H-NMR (400 MHz, $CDCl_3$) δ: 1.44 (9H, s), 2.85 (3H, s), 3.09–3.16 (1H, m), 3.39–3.46 (1H, m), 5.01–5.06 (1H, m), 7.24–7.34 (5H, m), 7.53 (1H, t, J = 7.0 Hz), 7.62 (1H, t, J = 7.4 Hz), 7.79 (1H, d, J = 8.2 Hz), 8.03 (1H, d, J = 8.2 Hz), 8.67 (1H, s), 8.73 (1H, s), 8.91 (1H, s); MS (APCI/ESI) m/z: 406 $[M+H]^+$; *Anal.* calcd for $C_{24}H_{27}N_3O_3 \cdot 0.40H_2O$: C, 69.85; H, 6.79; N, 10.18. Found C, 69.92; H, 6.74; N, 10.33; $[\alpha]_D^{25}$ +64.7 (c = 1.001, $CHCl_3$).

2-Benzyl-N4-*tert*-butyl-N1-(quinolin-3-yl)butanediamide (2e) Prepared as a mixture of conformers according to General Procedure A utilizing CH_2Cl_2 as a solvent. Yield: 69%. MS (APCI/ESI) m/z: 390 $[M+H]^+$; *Anal.* calcd for $C_{24}H_{27}N_3O_2 \cdot 0.20H_2O$: C, 73.33; H, 7.03; N, 10.69. Found C, 73.33; H, 7.01; N, 10.59.

***Nα*-(3,3-Dimethylbutanoyl)-*N*-quinolin-3-yl-D-phenylalaninamide (2f)** Prepared as a mixture of conformers according to General Procedure B utilizing 3,3-dimethylbutanoyl chloride as an acylating reagent. Yield: 88%. MS (APCI/ESI) m/z: 390 $[M+H]^+$; *Anal.* calcd for $C_{24}H_{27}N_3O_2 \cdot 0.30H_2O$: C, 73.00; H, 7.04; N, 10.64. Found C, 73.11; H, 7.01; N, 10.64; $[\alpha]_D^{25}$ +12.7 (c = 1.008, $CHCl_3$).

2-Benzyl-*N*-(2,2-dimethylpropyl)-*N*′-(quinolin-3-yl)propanediamide (2g) Prepared according to General Procedure A utilizing CH_2Cl_2 as a solvent. Yield: 63%. ^{1}H-NMR (400 MHz, $CDCl_3$) δ: 0.85 (9H, s), 3.02 (1H, dd, J = 6.1, 13.1 Hz), 3.09 (1H, dd, J = 6.7, 13.3 Hz), 3.27 (1H, dd, J = 8.6, 13.7 Hz), 3.36 (1H, dd, J = 7.0, 13.7 Hz), 3.64 (1H, t, J = 7.6 Hz), 6.89 (1H, t, J = 5.9 Hz), 7.06–7.27 (5H, m), 7.53 (1H, t, J = 7.2 Hz), 7.63 (1H, t, J = 7.0 Hz), 7.77 (1H, d, J = 7.8 Hz), 8.04 (1H, d, J = 8.6 Hz), 8.64 (1H, d, J = 2.3 Hz), 8.76 (1H, d, J = 2.7 Hz), 10.08 (1H, s); MS (APCI/ESI) m/z: 390 $[M+H]^+$; *Anal.* calcd for $C_{24}H_{27}N_3O_2 \cdot 0.20H_2O$: C, 73.33; H, 7.03; N, 10.69. Found C, 73.29; H, 7.02; N, 10.66.

***α*-(*tert*-Butylcarbamoyl)-*N*-quinolin-3-yl-D-phenylalaninamide (2h)** A solution of amine **3** (52 mg, 0.18 mmol) and *tert*-butylisocyanate (40 μL, 0.36 mmol) in toluene (2.3 mL) was stirred at room temperature for 18 h under N_2. The mixture was directly purified by silica gel chromatography to obtain **2h** (54.1 mg, 77%) as a mixture of conformers. MS (APCI/ESI) m/z: 391 $[M+H]^+$; *Anal.* calcd for $C_{23}H_{26}N_4O_2 \cdot 0.20H_2O$: C, 70.10; H, 6.75; N, 14.22. Found C, 69.95; H, 6.73; N, 14.19; $[\alpha]_D^{25}$ +6.1 (c = 1.010, $CHCl_3$).

(2*R*)-1-Oxo-3-phenyl-1-(quinolin-3-ylamino)propan-2-yl-*tert*-butylcarbamate (2i) A solution of 3-aminoquinoline (7.21 g, 50.0 mmol), **11** (13.3 g, 50.0 mmol) and HATU (19.01 g, 50.0 mmol) in *N*,*N*-dimethylformamide (DMF) (100 mL) was stirred at room temperature for 18 h under N_2. Water was added to the reaction mixture, and the mixture was extracted several times with EtOAc. The combined organic layer was dried over anhydrous Na_2SO_4 and concentrated under reduced pressure. The residue was purified by silica gel chromatography (hexane/EtOAc, 50 : 50) to obtain **2i** (8.70 g, 45%). ^{1}H-NMR (400 MHz, $CDCl_3$) δ: 1.33 (9H, s), 3.25 (1H, dd, J = 6.8, 14.2 Hz), 3.35 (1H, dd, J = 5.6, 13.9 Hz), 4.85 (1H, s), 5.49 (1H, t, J = 5.6 Hz), 7.23–7.30 (5H, m), 7.54 (1H, t, J = 7.6 Hz), 7.64 (1H, t, J = 7.6 Hz), 7.81 (1H, d, J = 7.8 Hz), 7.98 (1H, s), 8.03 (1H, d, J = 8.3 Hz), 8.55 (1H, d, J = 2.4 Hz), 8.72 (1H, d, J = 2.4 Hz); HRMS (ESI) m/z: $[M+H]^+$ calcd for $C_{23}H_{26}N_3O_3$, 392.1980; found 392.1983; *Anal.* calcd for $C_{23}H_{25}N_3O_3$: C, 70.57; H, 6.44; N, 10.73. Found C, 70.61; H, 6.28; N, 10.72. $[\alpha]_D^{25}$ +76.8 (c = 1.001, $CHCl_3$).

2-Methyl-6-nitro[1,3]thiazolo[5,4-*b*]pyridine (6)[22] A solution of 2-chloro-3,5-dinitropyridine (**5**, 1.00 g, 4.91 mmol) and thioacetamide (1.48 g, 19.7 mmol) in 1,4-dioxane (10 mL) was stirred at 100°C for 1 h. After the addition of water the mixture was extracted with EtOAc twice. The combined organic layers were dried over anhydrous Na_2SO_4 and concentrated under reduced pressure. The residue was purified by silica gel chromatography (hexane/EtOAc, 80 : 20) to obtain **6** (0.26 g, 27%) as a colorless solid. ^{1}H-NMR (400 MHz, DMSO-d_6) δ: 2.93 (3H, s), 9.06 (1H, d, J = 2.7 Hz), 9.38 (1H, d, J = 2.7 Hz).

2-Methyl[1,3]thiazolo[5,4-*b*]pyridin-6-amine HCl (7) A solution of **6** (0.26 g, 1.33 mmol), iron powder (1.49 g, 26.6 mmol) and 12 M HCl (70 μL) in water (2.7 mL) and EtOH (13 mL) was stirred at room temperature for 2 h. The reaction mixture was filtered through a pad of Celite, and the filtrate

was concentrated under reduced pressure to obtain crude **7**, which was used directly for the next reaction without further purification.

***N*-Quinolin-3-yl-D-phenylalaninamide (8)** A solution of **1c** (1.20 g, 3.07 mmol) and TFA (6.0 mL) in CH_2Cl_2 (30 mL) was stirred at room temperature for 3 h. After the addition of saturated aqueous solution of $NaHCO_3$ (pH = 10), the mixture was extracted with CH_2Cl_2 twice. The combined organic layers were dried over anhydrous Na_2SO_4 and concentrated under reduced pressure to obtain **8** (0.89 g, 99%). ^{1}H-NMR (400 MHz, $CDCl_3$) δ: 2.88 (1H, dd, J = 9.4, 14.1 Hz), 3.41 (1H, dd, J = 4.1, 13.9 Hz), 3.83 (1H, dd, J = 3.9, 9.4 Hz), 7.26–7.30 (3H, m), 7.34–7.37 (2H, m), 7.52–7.56 (1H, m), 7.61–7.66 (1H, m), 7.83 (1H, dd, J = 1.4, 8.0 Hz), 8.05 (1H, d, J = 8.2 Hz), 8.76 (1H, d, J = 2.3 Hz), 8.87 (1H, d, J = 2.3 Hz), 9.80 (1H, s).

Benzyl 3-Phenylpropanoate (10) A solution of benzyl 3-phenylpropanoyl chloride (**4**, 3.0 g, 17.8 mmol), Et_3N (3.0 mL, 21.5 mmol) and BnOH (2.0 g, 18.5 mmol) in CH_2Cl_2 (40 mL) was stirred at room temperature for 2 h. Water was added to the reaction mixture, and the mixture was extracted with EtOAc twice. The combined organic layer was dried over anhydrous Na_2SO_4 and concentrated under reduced pressure. The residue was purified by silica gel chromatography (hexane/EtOAc, 90 : 10) to obtain **10** (3.90 g, 91%). ^{1}H-NMR (400 MHz, $CDCl_3$) δ: 2.69 (2H, t, J = 7.4 Hz), 2.97 (2H, t, J = 7.8 Hz), 5.11 (2H, s), 7.17–7.37 (10H, m).

1-Benzyl 4-*tert*-Butyl 2-Benzylbutanedioate (11) *n*-BuLi (1.57 mmol/L in THF solution, 12.5 mL, 19.6 mmol) was added to a solution of *i*Pr_2NH (2.75 mL, 19.5 mmol) in THF (50 mL) at 0°C under N_2. After being stirred for 20 min at 0°C, THF (20 mL) solution of **10** (3.90 g, 16.2 mmol) was added to the reaction mixture at −78°C, and the mixture was stirred at −78 0°C for 30 min. THF (10 mL) solution of *tert*-butyl bromoacetate (4.40 g, 22.6 mmol) was added to the reaction mixture at −78°C, and the mixture was stirred at 0°C for 2 h. Saturated aqueous solution of NH_4Cl was added to the reaction mixture at 0°C, followed by extraction with EtOAc twice. The combined organic layers were washed with water, dried over anhydrous Na_2SO_4, and concentrated under reduced pressure. The residue was purified by silica gel chromatography (hexane/EtOAc, 90 : 10) to obtain **11** (3.29 g, 56%) as a colorless oil. ^{1}H-NMR (400 MHz, $CDCl_3$) δ: 1.39 (9H, s), 2.35 (1H, dd, J = 5.1, 16.4 Hz), 2.60 (1H, dd, J = 8.6, 16.4 Hz), 2.75–2.82 (1H, m), 3.02 (1H, dd, J = 6.7, 13.7 Hz), 3.12–3.14 (1H, m), 5.06 (1H, d, J = 12.5 Hz), 5.11 (1H, d, J = 12.5 Hz), 7.03–7.37 (10H, m).

3-Benzyl-4-(benzyloxy)-4-oxobutanoic Acid (12)[23] A solution of **11** (1.60 g, 4.51 mmol) and TFA (15 mL) in CH_2Cl_2 (15 mL) was stirred at room temperature for 18 h. After concentration of the reaction mixture, the mixture was purified by silica gel chromatography (CH_2Cl_2/MeOH, 90 : 10) to obtain **12** (970 mg, 72%) as a colorless oil. ^{1}H-NMR (400 MHz, $CDCl_3$) δ: 2.46 (1H, dd, J = 5.1, 17.2 Hz), 2.73 (1H, dd, J = 9.8, 17.2 Hz), 2.79 (1H, dd, J = 8.2, 13.7 Hz), 3.07 (1H, dd, J = 6.3, 13.7 Hz), 3.13–3.20 (1H, m), 5.10 (2H, s), 7.11–7.36 (10H, m).

Benzyl 2-Benzyl-4-(*tert*-butylamino)-4-oxobutanoate (13) Prepared according to General Procedure A utilizing CH_2Cl_2 as a solvent. Yield: 85%. ^{1}H-NMR (500 MHz, $CDCl_3$) δ: 1.28 (9H, s), 2.20 (1H, dd, J = 4.9, 14.2 Hz), 2.40 (1H, dd, J = 9.0, 14.9 Hz), 2.83 (1H, dd, J = 7.3, 12.7 Hz), 2.99 (1H, dd, J = 6.8, 13.7 Hz), 3.23–3.29 (1H, m), 5.06 (1H, d, J = 12.2 Hz), 5.11 (1H, d, J = 12.7 Hz), 5.26 (1H, s), 7.11–7.36 (10H, m).

2-Benzyl-4-(*tert*-butylamino)-4-oxobutanoic Acid (14) Prepared according to General Procedure C. Yield: 69%. ^{1}H-NMR (400 MHz, $CDCl_3$) δ: 1.33 (9H, s), 2.32–2.36 (2H, m), 2.77 (1H, dd, J = 9.2, 13.5 Hz), 3.09–3.23 (2H, m), 5.40 (1H, s), 7.18–7.33 (5H, m).

Benzyl 2-Benzyl-3-[(2,2-dimethylpropyl)amino]-3-oxopropanoate (16) Prepared according to General Procedure A utilizing CH_2Cl_2 as a solvent. Yield: 89%. ^{1}H-NMR (400 MHz, $CDCl_3$) δ: 0.81 (9H, s), 2.97 (1H, dd, J = 5.9, 13.3 Hz), 3.06 (1H, dd, J = 6.7, 13.3 Hz), 3.19 (1H, dd, J = 8.6, 13.7 Hz), 3.29 (1H, dd, J = 6.3, 13.7 Hz), 3.56 (1H, dd, J = 6.3, 8.6 Hz), 5.07 (2H, s), 6.45 (1H, s), 7.10–7.37 (10H, m).

2-Benzyl-3-[(2,2-dimethylpropyl)amino]-3-oxopropanoic Acid (17) Prepared according to General Procedure C. Yield: 99%. ^{1}H-NMR (400 MHz, $CDCl_3$) δ: 0.73 (9H, s), 2.83–2.94 (1H, m), 2.97–3.05 (1H, m), 3.12–3.20 (1H, m), 3.37–3.43 (2H, m), 5.56 (1H, s), 7.22–7.35 (5H, m).

(2*R*)-2-[(*tert*-Butylcarbamoyl)oxy]-3-phenylpropanoic Acid (20) Me_3SiCl (15.8 mL, 125 mmol) was added to a solution of benzyl (2R)-2-hydroxy-3-phenylpropanoate (18, 14.50 g, 56.7 mmol) and *tert*-butylisocyanate (15.8 mL, 125 mmol) in CH_2Cl_2 (300 mL) at room temperature under N_2. After the reaction mixture was stirred at room temperature for 18 h, the mixture was concentrated to obtain crude **19**. A solution of crude **19** and Pd/C (10%, 6.03 g) in EtOH (200 mL) was stirred at room temperature under H_2 for 2 h. After the removal of the catalyst, the residue was concentrated to obtain **20** (15.0 g, 99%, 2 steps) as a white powder. ^{1}H-NMR (500 MHz, $CDCl_3$) δ: 1.28 (9H, s), 3.07–3.13 (1H, m), 3.21 (1H, d, J = 15.1 Hz), 4.81 (1H, s), 5.22 (1H, s), 7.24–7.33 (5H, m).

High Throughput Electrophysiological Evaluation[26] The IonWorks Quattro system (version 2.0, Molecular Devices) was used for electrophysiological recordings. A 384-well plate containing the compounds to be tested was placed in the plate-1 position. A PatchPlate was clamped into the PatchPlate station. Once the experiment was started, the fluidics-head (F-head) added 3.5 μL of Dulbecco's Phosphate Buffered Saline (DPBS, with calcium and magnesium, Sigma-Aldrich Co. LLC) to each well of the PatchPlate and its underside was perfused with internal solution that had the following composition (in mM): 100.0 potassium D-gluconate, 40.0 KCl, 3.2 $MgCl_2$, 5.0 ethylene glycol bis(2-aminoethyl ether)-*N*,*N*,*N*′,*N*′-tetraacetic acid (EGTA), 5.0 *N*-(2-hydroxyethyl)piperazine-*N*′-2-ethanesulfonic acid (HEPES) (pH 7.27 using 1 M KOH). After priming and debubbling, the electronics-head (E-head) moved around the PatchPlate to perform a whole test. The F-head then dispensed 3.5 μL of the cell suspension ($hNa_V1.1/\beta1/\beta2$/HEK293A, $hNa_V1.5/\beta1/\beta2$/HEK293A, $hNa_V1.7/\beta1/\beta2$/HEK293A, $mNa_V1.1/\beta1/\beta2$/HEK293A, $mNa_V1.5/\beta1/\beta2$/HEK293A, or $mNa_V1.7/\beta1/\beta2$/HEK293A) into each well of the PatchPlate, and the cells were given 400 s to reach and seal the hole in each well. After this, the E-head moved around the PatchPlate to determine the seal resistance obtained in each well. Then, the solution on the underside of the PatchPlate was changed to access solution that had the following composition (in mM): 100.0 potassium D-gluconate, 40.0 KCl, 3.2 $MgCl_2$, 5.0 EGTA, 5.0 HEPES (pH 7.27 using 1 M KOH) plus 100 μg/mL of amphotericin B (Sigma-Aldrich Co. LLC.). After 10 min of patch perforation was allowed to take place, the E-head moved around the PatchPlate to obtain Na_V current measurements.

Table 5. Voltage Program

	$hNa_V1.1^{a)}$	$hNa_V1.5^{a)}$	$hNa_V1.7^{a)}$	$hNa_V1.7^{b)}$	$mNa_V1.1^{a)}$	$mNa_V1.5^{a)}$	$mNa_V1.7^{a)}$	$mNa_V1.7^{b)}$
Holding pulse (for 5 s)	−100 mV	−120 mV	−100 mV	−100 mV	−100 mV	−120 mV	−100 mV	−100 mV
Second conditioning pulse (for 2 s[a] or 10 s[b])	−43 mV	−68 mV	−59 mV	−30 mV	−44 mV	−69 mV	−56 mV	−30 mV
Holding pulse (for 50 ms)				−100 mV				−100 mV
Hyperpolarizing pulse (for 20 ms)				−140 mV				−140 mV
Test pulse (for analysis of inactivated-state channels, for 50 ms	0 mV	−20 mV	−10 mV	−10 mV	0 mV	−20 mV	−10 mV	−10 mV

a) Half-inactivated state. *b*) V_{hold} −30 mV.

After these pre-compound measurements, the F-head added 3.5 μL of solution from each well of the compound plate to each well on the PatchPlate. After about 5.5 min of incubation, the E-head moved around the PatchPlate to obtain post-compound Na_V current measurements. The pre- and post-compound Na_V current amplitude were measured from the peak current response subtracting the baseline current. The degree of Na_V current block was corrected by vehicle control currents as follows:

$$\%\ \text{inhibition} = 100 \times \left(\frac{1 - \text{relative current (compound)}}{\text{mean relative current (vehicle)}} \right)$$

where, relative current (compound) is the value of the post-compound Na_V current amplitude divided by the respective pre-compound Na_V current amplitude and mean relative current (vehicle) is the mean value of the post-vehicle Na_V current amplitude divided by the pre-vehicle Na_V current amplitude.

Data was fitted with a four parameter logistic equation:

$$Y = \text{Bottom} + (\text{Top} - \text{Bottom}) / (1 + 10^{[(\text{Log IC}_{50} - X) \times \text{HillSlope}]})$$

The voltage program for each Na_V subtype or species is summarized in Table 5.

PAMPA, Solubility, and Protein Binding Assay Each assay was performed as previously described.[27),28)]

Mouse PK Study All experimental procedures were performed in accordance with the in-house guideline of the Institutional Animal Care and Use Committee of Daiichi Sankyo Co., Ltd. For the determination of test compound exposures in male ddY mice, blood samples were collected at several timepoints post-dose. The plasma was separated from the blood by centrifugation, and stored at −70°C until use for the measurement of plasma concentration. The determination of the plasma concentration of the compound was performed by LC-MS/MS using API 4000 (Applied Biosystems/MDS SCIEX). PK parameters were calculated using a non-compartmental analysis techniques.

PSL Model in Mice All experimental procedures were performed in accordance with the in-house guideline of the Institutional Animal Care and Use Committee of Daiichi Sankyo Co., Ltd. Four-week-old PSL mice were purchased from Japan SLC, Inc., and were fed until 5 weeks old. The paw withdrawal latency (second) in each animal was measured at 0 (before administration) and at 30, 60, 120 and 180 min after administration in a blinded fashion. A planta thermal-stimulation device (PAW THERMAL STIMULATOR, UCSD, San Diego, CA, U.S.A.) was used for measurement. A 20 s cut-off time was employed to avoid tissue damage. No animal reached the cutoff value. The measurement was conducted after the animal placed in the measuring cage became calm. The value indicated by the device was transcribed to the recording sheet, and this value was used as the pain threshold.

Rotarod Performance in Mice All experimental procedures were performed in accordance with the in-house guideline of the Institutional Animal Care and Use Committee of Daiichi Sankyo Co., Ltd. ddY Mice able to walk on the rotarod (20 rpm, 3 cm in diameter; model MK-660C; Muromachi Kikai Co., Ltd., Tokyo, Japan) for 2 min were selected. After oral administration of the test compound or vehicle (control), each mouse was placed on the rotarod, and motor coordination was considered to be impaired if the rat fell off the rotarod within 120 s in two trials. The rotarod test was conducted at 0, 30, 60, and 120 min after administration.

Conflict of Interest Kyosuke Tanaka, Hiroyuki Kobayashi, Sayaka Suzuki, Satoshi Shibuya, Yuki Domon, Kazufumi Kubota, Yutaka Kitano, Chie Fujiwara, Daigo Asano, and Tsuyoshi Shinozuka are currently employees of Daiichi Sankyo Co., Ltd. Ryuta Koishi is currently employees of Daiichi Sankyo RD Novare Co., Ltd.

Supplementary Materials The online version of this article contains supplementary materials.

1. Eurofins Lead Profiling Data
2. Time course of antihyperalgesic effect of compounds **1c** and **1d**

References and Notes

1) Albers J. W., Pop-Busui R., *Curr. Neurol. Neurosci. Rep.*, **14**, 473 (2014).
2) Dworkin R. H., O'Connor A. B., Backonja M., Farrar J. T., Finnerup N. B., Jensen T. S., Kalso E. A., Loeser J. D., Miaskowski C., Nurmikko T. J., Portenoy R. K., Rice A. S., Stacey B. R., Treede R. D., Turk D. C., Wallace M. S., *Pain*, **132**, 237–251 (2007).
3) Cox J. J., Reimann F., Nicholas A. K., Thornton G., Roberts E., Springell K., Karbani G., Jafri H., Mannan J., Raashid Y., Al-Gazali L., Hamamy H., Valente E. M., Gorman S., Williams R., McHale D. P., Wood J. N., Gribble F. M., Woods C. G., *Nature* (London), **444**, 894–898 (2006).
4) Minett M. S., Nassar M. A., Clark A. K., Passmore G., Dickenson A. H., Wang F., Malcangio M., Wood J. N., *Nat. Commun.*, **3**, 791 (2012).
5) Eijkelkamp N., Linley J. E., Baker M. D., Minett M. S., Cregg R., Werdehausen R., Rugiero F., Wood J. N., *Brain*, **135**, 2585–2612 (2012).
6) Schmunk G., Gargus J. J., *Front. Genet.*, **4**, 222 (2013).
7) Catterall W. A., Goldin A. L., Waxman S. G., *Pharmacol. Rev.*, **57**, 397–409 (2005).
8) Bagal S. K., Chapman M. L., Marron B. E., Prime R., Storer R. I., Swain N. A., *Bioorg. Med. Chem. Lett.*, **24**, 3690–3699 (2014).
9) Nardi A., Damann N., Hertrampf T., Kless A., *ChemMedChem*, **7**,

1712–1740 (2012).
10) Bagal S. K., Brown A. D., Cox P. J., Omoto K., Owen R. M., Pryde D. C., Sidders B., Skerratt S. E., Stevens E. B., Storer R. I., Swain N. A., *J. Med. Chem.*, **56**, 593–624 (2013).
11) Suzuki S., Kuroda T., Kimoto H., Domon Y., Kubota K., Kitano Y., Yokoyama T., Shimizugawa A., Sugita R., Koishi R., Asano D., Tamaki K., Shinozuka T., Kobayashi H., *Bioorg. Med. Chem. Lett.*, **25**, 5419–5423 (2015).
12) Hoyt S. B., London C., Gorin D., Wyvratt M. J., Fisher M. H., Abbadie C., Felix J. P., Garcia M. L., Li X., Lyons K. A., McGowan E., MacIntyre D. E., Martin W. J., Priest B. T., Ritter A., Smith M. M., Warren V. A., Williams B. S., Kaczorowski G. J., Parsons W. H., *Bioorg. Med. Chem. Lett.*, **17**, 4630–4634 (2007).
13) Williams B. S., Felix J. P., Priest B. T., Brochu R. M., Dai K., Hoyt S. B., London C., Tang Y. S., Duffy J. L., Parsons W. H., Kaczorowski G. J., Garcia M. L., *Biochemistry*, **46**, 14693–14703 (2007).
14) Schenkel L. B., DiMauro E. F., Nguyen H. N., Chakka N., Du B., Foti R. S., Guzman-Perez A., Jarosh M., La D. S., Ligutti J., Milgram B. C., Moyer B. D., Peterson E. A., Roberts J., Yu V. L., Weisset M. M., *Bioorg. Med. Chem. Lett.*, **27**, 3817–3824 (2017).
15) Bedi S. S., Yang Q., Crook R. J., Du J., Wu Z., Fishman H. M., Grill R. J., Carlton S. M., Walters E. T., *J. Neurosci.*, **30**, 14870–14882 (2010).
16) Ma C., LaMotte R. H. J., *Neurosci.*, **27**, 14059–14068 (2007).
17) Sapunar D., Ljubkovic M., Lirk P., McCallum J. B., Hogan Q. H., *Anesthesiology*, **103**, 360–376 (2005).
18) Zhang X.-F., Zhu C. Z., Thimmapaya R., Choi W. S., Honore P., Scott V. E., Kroeger P. E., Sullivan J. P., Faltynek C. R., Gopalakrishnan M., Shieh C. C., *Brain Res.*, **1009**, 147–158 (2004).
19) Rogawski M. A., Tofighy A., White H. S., Matagne A., Wolff C., *Epilepsy Res.*, **110**, 189–205 (2015).
20) Compound **2i** inhibited rat $Na_V1.7$ at $IC_{50} = 47.9\,\mu M$ at V_{hold} −30 mV.
21) Seltzer Z., Dubnerb R., Shirc Y., *Pain*, **43**, 205–218 (1990).
22) Eurofin's Pan Labs lead profiling screen. This battery of radioligand binding assays consists of 67 common GPCRs, ion channels, and transporters, see Supporting Information for complete results.
23) Sahasrabudhe K. P., Estiarte M. A., Tan D., Zipfel S., Cox M., O'Mahony D. J. R., Edwards W. T., Duncton M. A. J., *J. Heterocycl. Chem.*, **46**, 1125–1131 (2009).
24) Plattner J. J., Marcotte P. A., Kleinert H. D., Stein H. H., Greer J., Bolis G., Fung A. K. L., Bopp B. A., Luly J. R., Sharn H. L., Kempf D. J., Rosenberg S. H., Dellaria J. F., Merits I., Perun T. J., *J. Med. Chem.*, **31**, 2277–2288 (1988).
25) Chorev M., Rubini E., Gilon C., Wormser U., Selinger Z., *J. Med. Chem.*, **26**, 129–135 (1983).
26) Finkel A., Wittel A., Yang N., Handran S., Hughes J., Costantin J., *J. Biomol. Screen.*, **11**, 488–496 (2006).
27) Shinozuka T., Tsukada T., Fujii K., Tokumaru E., Matsui Y., Wakimoto S., Ogata T., Araki K., Sawamura R., Watanabe N., Mori M., Tanaka J., *ACS Med. Chem. Lett.*, **10**, 358–362 (2019).
28) Nagata T., Yoshino T., Haginoya N., Yoshikawa K., Nagamochi M., Kobayashi S., Komoriya S., Yokomizo A., Muto R., Yamaguchi M., Osanai K., Suzuki M., Kanno H., *Bioorg. Med. Chem.*, **17**, 1193–1206 (2009).